

log resonances and in the fission process.

We thank H. Paetz gen. Schieck for his permanent help in running the Universität Köln polarized ion source even if only for an unpolarized beam. This work was supported in part by the Bundesministerium für Forschung und Technologie, Bonn, Germany.

<sup>1</sup>*Direct Interactions and Nuclear Reaction Mechanisms*, edited by E. Clementel and C. Villi (Gordon and Breach, New York, 1963), especially p. 382.

<sup>2</sup>S. Yoshida, *Annu. Rev. Nucl. Sci.* **24**, 1 (1974).

<sup>3</sup>W. M. Gibson, *Annu. Rev. Nucl. Sci.* **25**, 465 (1975).

<sup>4</sup>T. Ericson and T. Mayer-Kuckuk, *Annu. Rev. Nucl. Sci.* **16**, 183 (1966).

<sup>5</sup>K. A. Eberhard and A. Richter, in *Statistical Properties of Nuclei*, edited by J. B. Garg (Plenum, New York, 1972), p. 139.

<sup>6</sup>G. Ciocchetti and A. Molinari, *Nuovo Cimento* **40B**, 69 (1965).

<sup>7</sup>C. Maroni, I. Massa, and G. Vannini, *Phys. Lett.* **60B**, 344 (1976).

<sup>8</sup>J. S. Blair, P. Dyer, K. A. Snover, and T. A. Trainor, *Phys. Rev. Lett.* **41**, 1712 (1978).

<sup>9</sup>J. C. Hardy, J. A. Macdonald, H. Schmeing, H. R. Andrews, J. S. Geiger, R. L. Graham, T. Faestermann, E. T. H. Clifford, and K. P. Jackson, *Phys. Rev. Lett.* **37**, 133 (1976).

<sup>10</sup>J. H. Scofield, *Phys. Rev. A* **9**, 1041 (1974).

<sup>11</sup>W. Bambynek, B. Crasemann, R. W. Fink, H.-U. Freund, H. Mark, C. D. Swift, R. E. Price, and P. Venugopala Rao, *Rev. Mod. Phys.* **44**, 716 (1972).

<sup>12</sup>S. Hoppenau, Ph.D. thesis, Universität Köln, 1979 (unpublished).

<sup>13</sup>J. U. Andersen, E. Laegsgaard, M. Lund, C. D. Moak, and L. Kocbach, *J. Phys. B* **9**, 3247 (1976).

<sup>14</sup>M. Pauli, F. Rösel, and D. Trautmann, *J. Phys. B* **11**, 2511 (1978).

<sup>15</sup>M. Dost, S. Hoppenau, J. Kising, and S. Röhl, in *Proceedings of the Eleventh International Conference on the Physics of Electronic and Atomic Collisions*, Kyoto, 1979, Abstracts of Papers (to be published), p. 680.

## Angular Momentum Transfer in Incomplete-Fusion Reactions

K. A. Geoffroy and D. G. Sarantites

*Department of Chemistry, Washington University, St. Louis, Missouri 63130*

and

M. L. Halbert, D. C. Hensley, and R. A. Dayras<sup>(a)</sup>

*Oak Ridge National Laboratory, Oak Ridge, Tennessee 37830*

and

J. H. Barker

*Department of Physics, St. Louis University, St. Louis, Missouri 63103*

(Received 11 June 1979)

The measured correlation of charged-particle energies and angles with  $\gamma$ -ray multiplicities indicate that the average angular momentum transferred in the capture of  ${}^4\text{He}$ ,  ${}^8\text{Be}$ , and  ${}^{12}\text{C}$  from 153-MeV  ${}^{16}\text{O}$  projectiles by a  ${}^{154}\text{Sm}$  target increases linearly with captured mass. These incomplete-fusion processes are shown to originate from undamped peripheral collisions.

It has been known for some time<sup>1,2</sup> that in heavy-ion reactions energetic light charged particles are produced in larger yield than predicted by the evaporation theory and that they have forward-peaked distributions. Recent measurements<sup>3-5</sup> of  $\gamma$ -ray intensities in coincidence with high-energy  $\alpha$  particles at forward angles show a lack of side feeding to states with  $J^\pi \leq 10^+$ . These observations have been taken to indicate the existence of an incomplete fusion mechanism in heavy-ion reactions.<sup>3,4</sup> Excitation functions for ( ${}^{12}\text{C}, \alpha$ ) and

( ${}^{12}\text{C}, 2\alpha$ ) have been explained successfully in terms of successive critical angular momenta for various degrees of incomplete fusion.<sup>6</sup> All these results suggest but do not establish that this process occurs mainly for high  $l$  values in the entrance channel.

The experiment described here correlates energies and angles of charged particles from specific exit channels with  $\gamma$ -ray multiplicity and provides for the first time direct information on the angular momenta involved in various degrees

of incomplete fusion. We observe undamped collisions occurring with the capture by the target of the equivalent of one, two, or three  $\alpha$  particles from the  $^{16}\text{O}$ , and find a linear increase of the transferred angular momentum with captured mass. A simple interpretation of the results indicates that these processes are peripheral, with the highest entrance-channel ( $l$ ) values giving rise to the least-complete fusions.

A 153.0-MeV  $^{16}\text{O}$  beam from the Oak Ridge National Laboratory isochronous cyclotron bombarded a 1.3-mg/cm<sup>2</sup> target of  $^{154}\text{Sm}$  enriched to 98.69%. Six  $\Delta E \times E$  light-particle telescopes and seven 5.1-cm  $\times$  7.6-cm individually shielded NaI detectors<sup>7</sup> were operated in all possible coincidence modes with a 6.3% Ge(Li) detector at 45°. The telescopes were in the same plane as the Ge(Li) counter but on the opposite side of the beam at 10.5°, 25.5°, 45°, 80°, 120°, and 160° with half-angle acceptances of 1.4°, 4.1°, 6.7°, 6.7°, 6.7°, and 4.6°, respectively. The  $\Delta E$  counters were 26 to 73  $\mu\text{m}$  thick and the  $E$  counters 1500  $\mu\text{m}$  (2000  $\mu\text{m}$  at 10.5°).

The  $(\Delta E, E)$  maps of charged particles in coincidence with any Ge(Li) pulse are dominated by groups corresponding to each of the particle-stable isotopes of H, He, and Li. The 10.5° and 25° maps show also many particles with  $Z \geq 4$  whose spectra include substantial yields near the energy spectra corresponding to the beam velocity. For  $^{12}\text{C}$  most of the yield occurs in this region [Fig. 1(c)]; the same is true for  $^9,^{10}\text{Be}$ . This feature together with the strong forward peaking leads us to conclude that most of these particles are not due to deep-inelastic collisions.

The event tapes were scanned with  $(\Delta E, E)$  masks appropriate for various particle groups, producing Ge(Li) spectra in coincidence with specific numbers of NaI detectors. Selection of specific exit channels was achieved by choosing the known lines of various residual nuclei. Examples of the angular correlations between  $\gamma$  rays observed at 45° and  $\alpha$  particles at various angles and energies are shown in Fig. 1. For the lowest  $\alpha$ -particle energy bin in the reaction leading to  $^{159}\text{Er}$  [Fig. 1(a)], near symmetry about 90° is observed, characteristic of statistical emission from the compound nucleus,  $^{170}\text{Yb}$ . For higher  $E_\alpha$ , progressively stronger forward peaking is observed. Similar results are obtained for other  $^{166-x}\text{Er} + \alpha xn$  exit channels; the forward peaking is more pronounced for  $\alpha 6n$ , weaker for  $\alpha 8n$ , and very weak for  $\alpha 9n$ . If we decompose the angular correlations into two components, one of

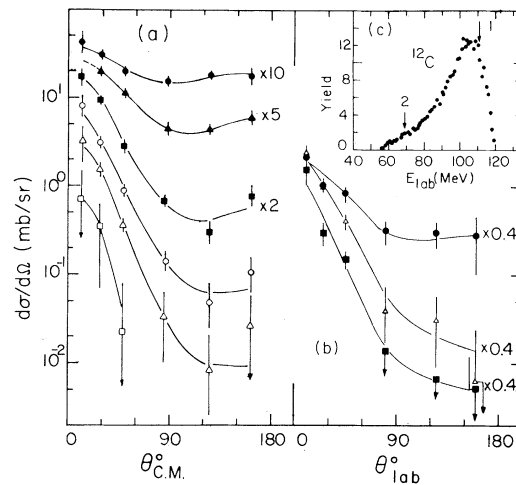


FIG. 1. (a) Angular correlation of  $\alpha$  particles coincident with known transitions in  $^{159}\text{Er}$  corresponding to  $\alpha n$  emission for various c.m.  $\alpha$ -particle energy bins (solid circles, 15–20 MeV; solid triangles, 20–25 MeV; solid squares, 25–30 MeV; open circles, 30–35 MeV; open triangles, 35–40 MeV; and open squares, 40–45 MeV). (b) Angular correlations of  $\alpha$  particles coincident with known transitions in  $^{157}\text{Dy}$  corresponding to emission of  $2\alpha + 5n$  (solid circles, 15–25 MeV; open triangles, 25–35 MeV; and solid squares, 35–60 MeV). (c) Spectrum of  $^{12}\text{C}$  particles at 25.5° in coincidence with any  $\gamma$  ray at 45°. Arrow 1 marks the energy corresponding to the projectile velocity. Arrow 2 shows the energy for a fully damped binary collision; the Coulomb energy was calculated with  $r_0 = 1.2$  fm.

them symmetric about 90° and containing all the 160° yield, we find that for  $E_\alpha = 35$ –40 MeV the asymmetric components in the four  $\alpha xn$  channels account for over 99% of the yield at 10.5°.

The correlations of  $\alpha$  particles coincident with several yrast transitions in  $^{156}\text{Dy}$  (emission of  $2\alpha + 5n$ ) are also strongly forward peaked [Fig. 1(b)]. Yields of  $^{156}\text{Dy}$  (emission of  $2\alpha + 6n$ ) are comparable and have similar correlations. Lines of  $^{154,155}\text{Gd}$  (emission of  $3\alpha + 4n$  or  $3\alpha + 3n$ ) were also seen, in coincidence with forward  $\alpha$  particles. Similar yields of  $^{150,151}\text{Sm}$  were observed in coincidence with forward  $\alpha$  particles.

The yields of Gd isotopes in coincidence with high-energy carbon ions are comparable to those in coincidence with  $\alpha$  particles. In contrast, the lines of  $^{156,157}\text{Dy}$  in coincidence with high-energy  $^9,^{10}\text{Be}$  ions have roughly 20% of the yield seen with the  $\alpha$  mask; it may be that much of the latter Dy yield actually results from  $^8\text{Be}$ . The angular correlations of Be and C in coincidence with Dy and Gd  $\gamma$  rays, respectively, are also forward

peaked. No significant yields of Sm were observed in coincidence with carbon.

Estimates of the angle-integrated cross sections of the asymmetric component for the strongest incomplete fusion exit channels are given in Table I. For comparison, the complete-fusion cross section is  $1200 \pm 150$  mb ( $I_{\text{fus}} = 60 \pm 4$ ), obtained from  $\gamma$ -ray yields of  $xn$  and  $\alpha xn$  evaporation residues in a companion experiment<sup>8</sup> at 156 MeV ( $1210 \pm 100$  mb, less  $\sim 220$  mb for incomplete fusion) plus estimates of the yields of  $pxn$  residues ( $\sim 150$  mb) and of fission ( $\sim 60$  mb from systematics<sup>9</sup>).

The average  $\gamma$ -ray multiplicity  $\langle M_\gamma \rangle$ , the standard deviation  $\sigma_\gamma$ , and the skewness  $s_\gamma$  were obtained in the usual way.<sup>7,10</sup> Because of limited statistics, the higher moments were not well defined unless sums over energy bins and/or over exit channels were used. Figure 2 shows  $\langle M_\gamma \rangle$ ,  $\sigma_\gamma$ , and  $s_\gamma$  for coincidences with  $\alpha$  particles at  $10.5^\circ$  without exit-channel selection. In view of the slight  $E_\alpha$  dependence displayed in Fig. 2,  $\langle M_\gamma \rangle$  and  $\sigma_\gamma$  for the  $\alpha 7n$  and  $\alpha 6n$  channels were calculated for  $E_\alpha > 25$  MeV from a smoothed plot of the fold distributions and are shown by the open points in Figs. 2(a) and 2(b); these come

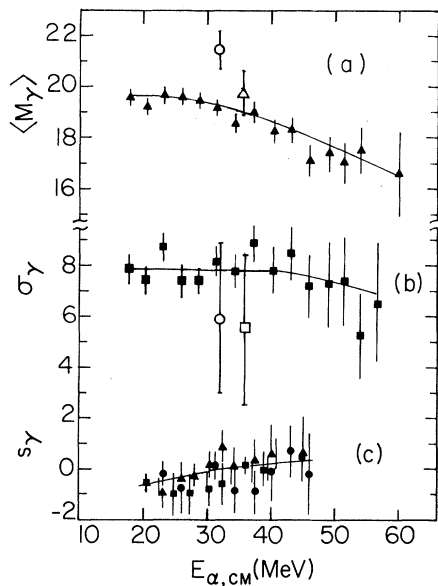


FIG. 2. (a)  $\langle M_\gamma \rangle$  vs  $E_{\alpha, c.m.}$  at  $10.5^\circ$  in coincidence with any  $\gamma$  ray (solid triangles). The open triangle and circle are for the  $\alpha 6n$  and  $\alpha 7n$  channels with  $E_\alpha > 25$  MeV. (b) Width  $\sigma_\gamma$  vs  $E_\alpha$  at  $10.5^\circ$  (solid squares). The open square and circle are for the  $\alpha 6n$  and  $\alpha 7n$  channels with  $E_\alpha > 25$  MeV. (c) Skewness  $s_\gamma$  vs  $E_\alpha$  at  $10.5^\circ$  (solid circles),  $25.5^\circ$  (solid squares), and  $45^\circ$  (solid triangles).

principally from the  $25.5^\circ$  counter.

Table I lists  $\langle M_\gamma \rangle$  and  $\sigma_\gamma$  for the products of incomplete fusion. Using transformations similar to those given in Ref. 10 for obtaining the distribution of  $J_\gamma$ , the angular momentum prior to  $\gamma$  decay, we find that the principal contributions for each process come from different regions in  $J_\gamma$  space. In particular, the less complete the fusion (i.e., the lighter the captured fragment from  $^{16}\text{O}$ ), the lower the angular momentum of the residual nucleus [Fig. 3(c)].

If the higher moments of the multiplicity distribution are known, the  $J_\gamma$  distribution may be constructed.<sup>10</sup> Figure 3(a) shows examples of such calculations for  $^{160}\text{Er}$ ,  $^{157}\text{Dy}$ , and  $^{154}\text{Gd}$  with  $\sigma_\gamma = 5.6$ ,  $4.7$ , and  $3.5$  (corresponding to full width at half maximum  $\sim 22\hbar$ ,  $\sim 18\hbar$ , and  $\sim 12\hbar$ ) and  $s_\gamma = 0.4$ ,  $0.6$ , and  $0.8$ , respectively. These values of  $\sigma_\gamma$  are based on the individual-channel data of Table I. The  $\sigma_\gamma$  values without exit-channel selection [Fig. 1(b), Table I] have much smaller uncertainties, but they cannot be used because they reflect broadening due to superposition of distributions from different regions of  $J$  space. The  $J_\gamma$  distributions of Fig. 3(a) are consistent with our observed side-feeding pattern to low- $J$

TABLE I. Cross sections  $\sigma$ , average multiplicities  $\langle M_\gamma \rangle$ , and widths  $\sigma_\gamma$  for products of incomplete fusion of 153-MeV  $^{16}\text{O}$  with  $^{154}\text{Sm}$ .

Final products <sup>a</sup>	$\sigma^b$	$\langle M_\gamma \rangle^c$	$\sigma_\gamma^c$
$^{159}\text{Er} + \underline{\alpha 7n}$	32, <u>5</u>	21.5, <u>8</u>	5.9, <u>30</u>
$^{160}\text{Er} + \underline{\alpha 6n}$	50, <u>7</u>	19.8, <u>9</u>	5.6, <u>30</u>
$^{156}\text{Dy} + \underline{2\alpha 6n}$	21, <u>3</u>	15.4, <u>30</u>	< 5
$^{157}\text{Dy} + \underline{2\alpha 5n}$	13, <u>2</u>	12.7, <u>17</u>	< 5
$^{153}\text{Gd} + \underline{\text{C}xn}$	7, <u>3</u>		
$^{154}\text{Gd} + \underline{\text{C}xn}$	35, <u>15</u>	11.0, <u>8</u>	< 4
$^{154}\text{Gd} + \underline{3\alpha 4n}$	18, <u>5</u>		
$^{155}\text{Gd} + \underline{\text{C}xn}$	15, <u>5</u>	12.4, <u>12</u>	< 4
$^{155}\text{Gd} + \underline{3\alpha 3n}$	11, <u>3</u>		
$^{156}\text{Gd} + \underline{\text{C}xn}$	23, <u>8</u>	10.3, <u>13</u>	< 4
$^{156}\text{Gd} + \underline{\alpha}^d$		19.1, <u>2</u>	7.7, <u>4</u>
$^{156}\text{Gd} + \underline{\text{C}}^e$		10.2, <u>6</u>	6.0, <u>6</u>

<sup>a</sup>The underlined particle was detected in coincidence with characteristic  $\gamma$  rays from the indicated nuclide.

<sup>b</sup>Angle-integrated cross sections in mb per product nuclide for the forward-peaked component only.

<sup>c</sup>For 25.5° particles of any energy (Dy or Gd) or  $E_\alpha > 25$  MeV (Er). (See also footnote a.)

<sup>d</sup>Coincidences with an  $\alpha$  particle above 25 MeV and any  $\gamma$  ray.

<sup>e</sup>Coincidences with any carbon particle and any  $\gamma$  ray.

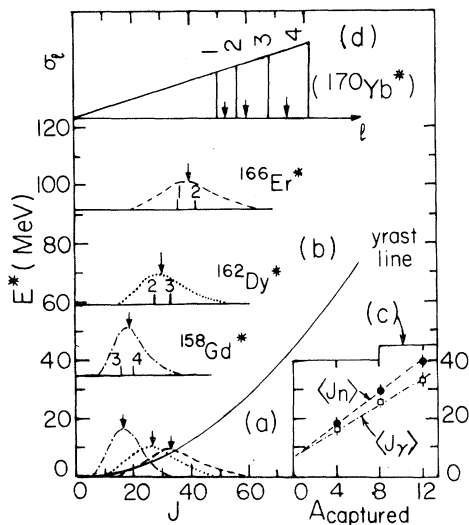


FIG. 3. (a) Entry-state  $J_\gamma$  distributions in  $^{160}\text{Er}$  (dashed curve),  $^{157}\text{Dy}$  (dotted curve), and  $^{154}\text{Gd}$  (dash-dotted curve) associated with energetic forward-emitted fragments. The vertical arrows give  $\langle J_\gamma \rangle$ . (b)  $J_n$  distributions prior to neutron emission leading to the same products. The vertical arrows indicate the  $\langle J_n \rangle$  values. The base-line ordinate for each  $J_n$  distribution represents the excitation energy of the product after emission of the appropriate projectile fragment(s) with the beam velocity. The yrast line is for a rigid sphere of  $A=162$  and  $r_0 = 1.2$  fm. (c) Plot of  $\langle J_\gamma \rangle$  and  $\langle J_n \rangle$  vs captured mass, assumed to be twice the captured charge. (d) Regions of incomplete fusion based on the model of Ref. 6. The vertical lines 1, 2, 3, and 4 give the critical  $l$  values for the onset of  $^{12}\text{C}$ ,  $^8\text{Be}$ ,  $^4\text{He}$  capture, and no capture ( $4\alpha$  breakup), respectively. The arrows show  $\langle l \rangle$  deduced from the present data.

states in the ground bands of the Er, Dy, and Gd products.

The average angular momentum prior to neutron emission,  $\langle J_n \rangle$ , was obtained by adding to  $\langle J_\gamma \rangle$   $0.6\hbar$  per emitted neutron for  $^{154}\text{Gd}$ ,  $0.8\hbar$  for  $^{157}\text{Dy}$ , and  $1.2\hbar$  for  $^{160}\text{Er}$ . Figure 3(b) shows  $J_n$  distributions constructed from these values of  $\langle J_n \rangle$  and with the same width and skewness as above. The average angular momentum transferred to the incompletely fused system increases linearly with the mass of the captured fragment as shown in Fig. 3(d). Assuming that the angular momentum of the initial system is divided between the projectile fragments in proportion to their masses, we find that  $\langle l \rangle$ , the average entrance-channel angular momentum quantum num-

ber, is 52, 60, and 74 for reactions involving the capture of  $^{12}\text{C}$ ,  $^8\text{Be}$ , and  $^4\text{He}$ , respectively. Figure 3(d) compares these  $\langle l \rangle$  values (denoted by arrows) with the  $l$  thresholds for the corresponding captures calculated according to the model of Ref. 6. As  $l$  increases, the competition from successively opened incomplete-fusion channels produces a maximum in the yield for each channel above its critical  $l$  value. The numbered markers in Fig. 3(b) show the corresponding threshold  $J$  values for the channel in question and the next one. The experimental  $\langle J_n \rangle$  values [arrows in Fig. 3(b)] fall between these limits.

In conclusion, we have established the following:

(1) Incomplete fusion of 153-MeV  $^{16}\text{O}$  with  $^{154}\text{Sm}$  occurs with significant cross section.

(2) The remnants of the projectile are emitted forward with velocities near that of the projectile.

(3) The average transferred angular momenta are nearly proportional to the captured mass. The entrance-channel  $\langle l \rangle$  values deduced for capture of  $^{12}\text{C}$ ,  $^8\text{Be}$ , and  $^4\text{He}$  are 52, 60, and 74, and increase as the captured mass decreases.

(4) The present results are consistent with the model of Siwek-Wilczyńska *et al.* (Ref. 6).

We wish to thank J. R. Beene and R. G. Stokstad for valuable discussions. This work was supported in part by the U. S. Department of Energy, Division of Basic Energy Sciences. Oak Ridge National Laboratory is operated by Union Carbide Corporation for the U. S. Department of Energy.

(a) Present address: Service de Physique Nucléaire, Centre d'Etudes de Bruyères-le-Châtel, Boîte Postale 561, 92542 Montrouge, France.

<sup>1</sup>H. C. Britt and A. R. Quinton, Phys. Rev. **124**, 877 (1961).

<sup>2</sup>J. Galin *et al.*, Phys. Rev. C **9**, 1126 (1974).

<sup>3</sup>T. Inamura *et al.*, Phys. Lett. **68B**, 51 (1977).

<sup>4</sup>D. R. Zolnowski *et al.*, Phys. Rev. Lett. **41**, 92 (1978).

<sup>5</sup>L. Westerberg *et al.*, Phys. Rev. C **18**, 796 (1978).

<sup>6</sup>K. Siwek-Wilczyńska *et al.*, Phys. Rev. Lett. **42**, 1599 (1979).

<sup>7</sup>L. Westerberg *et al.*, Nucl. Instrum. Methods **145**, 295 (1977).

<sup>8</sup>K. A. Geoffroy *et al.*, Bull. Am. Phys. Soc. **23**, 503 (1978).

<sup>9</sup>A. M. Zebelman *et al.*, Phys. Rev. C **10**, 200 (1974).

<sup>10</sup>D. G. Sarantites *et al.*, Phys. Rev. C **18**, 774 (1978).